Cation permeability of a cloned rat epithelial amiloride-sensitive Na$^+$ channel

Iskander I. Ismailov *†, Vadim Gh. Shlyonsky *, Osvaldo Alvarez ‡
and Dale J. Benos*

*Department of Physiology and Biophysics, University of Alabama at Birmingham,
Birmingham, AL 35294-0005, USA and ‡ Departamento de Biologia, Facultad de Ciencias,
Universidad de Chile, Casilla 653, Santiago, Chile*

1. Conductance of heterotrimeric rat epithelial Na$^+$ channels (α, β, γ-rENaCs) for Li$^+$ and Na$^+$ in planar lipid bilayers was a non-linear function of ion concentration, with a maximum of $30\cdot4 \pm 2\cdot9$ pS and $18\cdot5 \pm 1\cdot9$ pS at 1 M Li$^+$ and Na$^+$, respectively.

2. The α, β, γ-rENaC conductance measured in symmetrical mixtures of Na$^+$–Li$^+$ (1 M) exhibited an anomalous mole fraction dependence, with a minimum at 4:1 Li$^+$ to Na$^+$ molar ratio.

3. Permeability ratios P_K/P_{Na} and P_{Li}/P_{Na} of the channel calculated from the biionic reversal potentials were dependent on ion concentration: P_K/P_{Na} was $0\cdot11 \pm 0\cdot01$, and P_{Li}/P_{Na} was $1\cdot6 \pm 0\cdot3$ at 50 mM; P_K/P_{Na} was $0\cdot04 \pm 0\cdot01$ and P_{Li}/P_{Na} was $2\cdot5 \pm 0\cdot4$ at 3 M, but differed from the ratios of single-channel conductances in symmetrical Li$^+$, Na$^+$ or K$^+$ solutions. The permeability sequence determined by either method was Li$^+$ > Na$^+$ > K$^+$ $\gg$ Rb$^+$ > Cs$^+$.

4. Predictions of a model featuring two binding sites and three energy barriers (2S3B), and allowing double occupancy, developed on the basis of single ion current–voltage relationships, are in agreement with the observed conductance maximum in single ion experiments, conductance minimum in the mole fraction experiments, non-linearity of the current–voltage curves in biionic experiments, and the concentration dependence of permeability ratios.

5. Computer simulations using the 2S3B model recreate the ion concentration dependencies of single-channel conductance observed for the immunopurified bovine renal amiloride-sensitive Na$^+$ channel, and short-circuit current in frog skin, thus supporting the hypothesis that ENaCs form a core conduction unit of epithelial Na$^+$ channels.

Amiloride-sensitive Na$^+$ channels are the rate-limiting step for net Na$^+$ transport across reabsorbing epithelia such as renal distal and collecting tubules and distal colon, the ducts of several exocrine glands, and the lung. Renal reabsorption of sodium through this channel is one of the essential mechanisms involved in the regulation of sodium balance, blood volume, and blood pressure. Representatives of a family of these channels were first cloned from the rat colon (Canessa, Horisberger & Rossier, 1993; Lingueglia, Voilley, Waldman, Lazdunski & Barbry, 1993; Canessa *et al.* 1994), and subsequently from several other sources (Fuller *et al.* 1995; Puoti, May, Canessa, Horisberger, Schild & Rossier, 1995). Independent of their origin, these channels appear to be heteromeric and consist of at least three homologous subunits termed α-, β- and γ-ENaC (epithelial Na$^+$ channel). The α-ENaC subunit is a ∼700 residue polypeptide that has

at least two putative transmembrane segments. When β- and γ-subunits are co-expressed with α-ENaC, the *Xenopus* oocyte membrane reproduces faithfully many of the properties of amiloride-sensitive Na$^+$ channels found in native epithelia (Canessa *et al.* 1994). Polypeptides resulting from *in vitro* translation self-assemble into functional channels in liposomes, as demonstrated by reconstitution of these liposomes into planar lipid bilayers (Ismailov *et al.* 1996a). Criteria used to demonstrate that the observed channels were attributable to ENaC were a high-affinity amiloride blockade with an apparent equilibrium inhibitory dissociation constant ($K_{i,amil}$) of 170 nM, and a Na$^+$/K$^+$ permeability ratio of 10 (Ismailov *et al.* 1996). Therefore, ENaCs incorporated into planar lipid bilayers constitute an ideal model system in which to study biophysical processes underlying ion conduction through these channels. The aim

† To whom correspondence should be addressed at University of Alabama at Birmingham, Department of Physiology & Biophysics, 1918 University Boulevard - 705 BHSB, Birmingham, AL 35294-0005, USA.

of the present work was to examine systematically the monovalent cation permeability characteristics of the channel formed by association of rat ENaC (rENaC) α-, β- and γ-subunits. We also sought to develop a minimal model to account for the dependence of the conduction process on ion activity and applied voltage. We demonstrate that monovalent cation permeation through ENaC can be understood in terms of an energy barrier model featuring two binding sites and three barriers that allows multiple occupancy.

METHODS

Reagents

Phospholipids were purchased from Avanti Polar Lipids (Alabaster, AL, USA). Cholesterol was purchased from Sigma, and was oxidized by bubbling 100% O_2 through a 4% cholesterol in octane solution at the octane boiling point of 126 °C (Tien, Carbone & Dawidowicz, 1966) for 3 h. All other chemicals were reagent grade, and all solutions were made with distilled water and filter sterilized before use (Sterivex-GS, 0·22 μm filter, Millipore Corp., Bedford, MA, USA).

Translation, transcription, purification and self assembly of the channel

In vitro translation of individual α-, β- and γ-rENaC proteins was accomplished as described earlier (Ismailov *et al.* 1996*a*). Briefly, purified and linearized DNA plasmids encoding each subunit were *in vitro* transcribed using T7 RNA polymerase (Ribomax kit, Promega, Madison, WI, USA), according to the manufacturer's instructions. *In vitro* translations of individual subunits were carried out for 2 h at 30 °C, using a micrococcal nuclease-treated rabbit reticulocyte cell lysate (Promega, Madison, WI, USA) in the presence of canine microsomal membranes and 0·8 mCi ml^{-1} [^{35}S] *trans* label (ICN, Costa Mesa, CA, USA). A 25 μl translation reaction for each subunit was mixed with 0·5 mg phosphatidyl-ethanolamine (PE), 0·3 mg phosphatidylserine (PS), 0·2 mg phosphatidylcholine (PC), Triton X-100 (0·2% (v/v), final concentration), and 25 μl of a buffer containing 60 mM tris (hydroxymethyl) aminomethane (Tris; pH 6·8), and 25% glycerol (v/v). The translated α-, β- and γ-rENaC proteins were eluted from a G-150 superfine Sephadex (Pharmacia Biotech., Inc.) gel filtration column with a buffer containing 500 mM NaCl, 1 mM EDTA and 10 mM Tris (pH 7·6). The individual α-, β- and γ-rENaC proteins were mixed at a ratio of 1:1:1 based on the [^{35}S] measurements, assuming similar methionine/cysteine compositions for each subunit. Control liposomes were also prepared with mock *in vitro* translation/Sephadex purification products, following an identical protocol, but omitting rENaC mRNA.

Planar lipid bilayer experiments

Planar lipid bilayers were routinely painted with a fire-polished glass rod over an aperture of 200 μm diameter drilled in a polystyrene chamber. The membrane-forming solution consisted of a mixture of either diphytanoyl-phosphatidylethanolamine/diphytanoyl-phosphatidylserine/oxidized cholesterol or diphytanoyl-phosphatidyl-ethanolamine/diphytanoyl-phosphatidyl-choline/oxidized cholesterol 2:1:2 (w/w/w, final lipid concentration of 25 mg ml^{-1} in *n*-octane). A membrane capacitance of 300–400 pF (0·23–0·32 μF cm^{-2}) determined as a capacitive current in response to a triangular pulse was considered satisfactory for experimentation. The bilayer bathing solutions contained salt buffers of appropriate composition (see specific

experimental designs) with 10 mM Mops–Tris (pH 7·4). Single-channel currents were measured using a conventional current-to-voltage converter based on an OPA-101 (Burr-Brown, Tucson, AZ, USA) operational amplifier with a 10 GΩ feedback resistor. The current-to-voltage converter was connected to the *trans* side of the bilayer chamber using a Ag–AgCl electrode and 3 M KCl–3% agar bridges. Thus the *trans* compartment was made virtual ground. The *cis* compartment was connected to a voltage source using a Ag–AgCl electrode and 3 M KCl–3% agar bridge. α, β, γ-rENaCs were fused to the *trans* side of a pre-made bilayer (held at −40 mV) using a fire-polished glass rod dipped into a suspension of reconstituted proteoliposomes containing a mixture of *in vitro* translated α-, β- and γ-rENaC proteins. This protocol provided a specific sidedness to incorporation of the channels, i.e. they were oriented with the amiloride-sensitive (extracellular) side facing the *trans* solution and the cytoplasmic side facing the *cis* solution in over 90% of successful incorporations reported here (173 out of 192). The orientation of the channel in the membrane was determined by adding amiloride to one or other bathing solution. All experiments were performed at 25 ± 1 °C.

Currents were monitored on a strip chart recorder (EasyGraf Recorder TA 240, Gould Electronics) and/or a digital storage oscilloscope, and were stored unfiltered on a VCR tape using a Vetter model 20 digital data recorder (Vetter Instruments). Current records were low-pass filtered at the desired frequency through an 8-pole Bessel filter (902 LPF, Frequency Devices, Haverhill, MA, USA) prior to acquisition using a Digidata 1200 interface and pCLAMP 5.6 software (Axon Instruments).

Mole fraction experiments. Each experiment was initiated with symmetrical 100 mM (or 1 M) NaCl solutions in both compartments. Solutions containing mixtures of Li$^+$ and Na$^+$ at different molar ratios were prepared by substitution of an exactly measured volume of the NaCl bathing solution from both compartments of the bilayer chamber with exactly the same volume of 100 mM (or 1 M) LiCl solution. The maximal volume substituted did not exceed 10% of the total volume (i.e. 0·4 ml per chamber), in order to avoid breakage of the membrane. Solutions were stirred for 1 min. This protocol permitted conductance measurements of the same channel in solutions with different molar fractions of Li$^+$ and Na$^+$.

Liquid junction potential correction. Reversal potentials were corrected for liquid junction potentials (E_{LJ}) measured in each experiment under biionic conditions. The voltage across an ENaC-free membrane (bare bilayer) following replacement of the *cis* bathing solution with an appropriate salt concentration was measured by constructing a current–voltage curve under voltage clamp and interpolating for voltage at zero current conditions and subtracted from experimental values. The magnitude of this liquid junction potential varied from −3 to +6 mV for different biionic conditions.

Data analysis

Calculation of the unitary current. The unitary current (I) was determined from all-points current amplitude histograms produced by pCLAMP software based on the following considerations: (1) in all the experiments performed to date (over 2000) reported here and previously (see also Ismailov *et al.* 1996*a*; Ismailov, Berdiev, Shlyonsky & Benos, 1997*a*), α, β, γ-rENaC displayed a gating pattern of three equally spaced subconductive states (13, 26 and 39 pS at 100 mM NaCl); (2) the 13 pS and/or 26 pS transitions have never been observed independently of each other or of the third, highest conductance level. The total number of channels (N) present in the bilayer in each experiment was determined by activating all of them with a hydrostatic pressure gradient. This

procedure originated from previous observations that the channel open probability (P_o) approaches 1 when a sufficient hydrostatic pressure gradient is imposed across an ENaC-containing bilayer (Awayda, Ismailov, Berdiev & Benos, 1995; Ismailov *et al.* 1996*a*).

Calculation of the permeability ratios. The relative permeability of α, β, γ-rENaC for monovalent cations was calculated from the reversal (zero current) potentials measured under biionic conditions, using the Goldman–Hodgkin–Katz equation:

$$P_S/P_{Na} = ([Na]_{trans}\, a_{Na})/(z^2\, [S]_{cis}\, a_S) \exp(-zFE_{rev}/RT), \quad (1)$$

where P_{Na} and P_S are the permeabilities for Na⁺ and the test cation, respectively, E_{rev} is the reversal potential, a_{Na} and a_S are single ion activity coefficients, z is the valence of the test cation, and F, R and T have their usual thermodynamic meanings.

The reversal potentials were determined by approximation of the curves to the Goldman–Hodgkin–Katz current equation:

$$I = I_{Na} + I_S$$

$$I_{Na} = P_{Na}z\,(EF^2/RT)\,(-[Na^+]_{trans}\exp(-FE/RT))/(1 - \exp(-FE/RT))$$

$$I_S = P_S z\,(EF^2/RT)\,([S^+]_{cis}/(1 - \exp(-FE/RT))), \quad (2)$$

where I_{Na} and I_S are the fractions of the total current I carried by Na⁺ and the test cation at a given applied potential E, and ion concentrations in *trans* and *cis* compartments are $[Na^+]_{trans}$ and $[S^+]_{cis}$, respectively. P_{Na} and P_S are the permeabilities for Na⁺ and the test cation, respectively; z is the valence of the test cation, and F, R and T have their usual thermodynamic meanings.

The molar activity coefficients at given concentrations were obtained from Lide (1996). The single-ion activity coefficients for Na⁺, Li⁺ and K⁺ were assumed to be the same as the activity coefficients for the whole salt.

Modelling of energy profiles. Ion conduction was modelled as translocation over the energy barriers following Hille & Schwartz (1978), because this theory has been proven to be useful for explaining a variety of observed ion channel phenomena such as conductance saturation, inhibition and blockade, anomalous mole fraction effect, and concentration dependence of permeability ratios, all of which are displayed by the ENaC channel. The free energy at each of the wells and peaks consists of a voltage-independent component that represents interaction of the ion with the channel and a voltage-dependent component that is a linear function of the applied trans-membrane potential and an electrical distance. In order to calculate the free energy profile for the ion in the channel, currents through α, β, γ-rENaC measured under different ionic conditions were subjected to a non-linear curve-fitting procedure based on the Gauss–Newton method using the AJUSTE program (Alvarez, Villarroel & Eisenman, 1992) and a three-barrier–two-site (3B2S) channel model, which represents a minimal model allowing multiple occupancy. The function for this model includes six adjustable energy parameters: three peak energies (G1, G2 and G3), and two well energies (U1 and U2). It also includes five distance parameters (D1 to D5), referred to the fraction of the electric field that separates peak and well positions, with a requirement that the sum of all peak-to-well distances equals one. Because the model allows multiple occupancy, an ion–ion interaction parameter (A) is used to describe a shift in the energy of peaks and wells, when the channel is occupied (for example, as a consequence of the electric field around the ion). To describe such interactions, we assume that the energy shift is proportional to the inverse of the distance measured from the ion to any other point in the channel (Alvarez *et al.* 1992). These distance parameters are used in combination with the interaction parameter

A to calculate the energy shift. As an example, the energy shift of well j caused by an ion in well i is:

Energy shift of well $j = A/$(distance from well i to well j), (3*a*)

and the energy shift on peak j caused by an ion in well i is:

Energy shift of peak $j = A/$(distance from well i to peak j). (3*b*)

Rate constants describing ion translocation from one well to another were calculated as:

Rate constant =

$\quad (k\,(T/h))\exp(-1\,(((\text{barrier height} - \text{well depth})/RT))), \quad (4)$

where k is the Boltzmann constant, T is the absolute temperature and h is the Planck constant). The single-channel current measured at a given holding potential is related to the net ion transport rate (sum of the differences between the backward and forward rates) in the channel as a product of this rate and the electron charge.

The probability of occupancy of each well was calculated for the steady-state condition, and the rate of hopping between wells was calculated as the product of the probability of occupancy of the well times the appropriate rate constant. The best-fit parameter values were searched for by the AJUSTE program, which minimizes the weighted sum of squares of the differences between experimental and theoretical data. The weight factors were set as inverse for each current value unless otherwise stated. The single ion activities were used for all computations, but ion concentrations were used in the text and all figures for ease of discussion. A hypothetical solution of a mole fraction of 1 was used as the reference state for the ions in solution. Statistical analyses of the correlation between the experimental and theoretically predicted data points were performed using SigmaStat software (Jandel Scientific, San Rafael, CA, USA).

RESULTS

Conductance properties of α, β, γ-rENaC for a single permeant ion

The first aim of this study was to determine the conduction properties of α, β, γ-rENaC following incorporation in planar lipid bilayer membranes. *In vitro* translated α, β, γ-rENaC was incorporated into bilayers bathed with symmetrical solutions containing chloride salts of the monovalent metal cations. When bathed with symmetrical 10 mM NaCl buffers, α, β, γ-rENaC resided primarily in a 3 pS conductance sublevel with brief openings to a 9 pS level. This type of concerted gating behaviour was consistent with our previous observations of three equally spaced states of conductance (0: closed; 1, 2 and 3: open) in α, β, γ-rENaC when the current intensity displayed frequent transitions from state 1 to state 3, skipping state 2 (Ismailov *et al.* 1996*a*); the phenomenon was considered as implying simultaneous openings of two ion conduction pathways, and suggestive of a multimeric organization of α, β, γ-rENaC. Symmetrically elevating the salt concentration in both bathing solutions resulted in an increase in the conductance of the channel and, at higher concentrations, in the appearance of three equally spaced subconductive states (Fig. 1), consistent with the previously reported triple barrel organization of α, β, γ-rENaC (Ismailov *et al.* 1996*a*). An essentially identical type of channel gating was observed in 10 mM–3 M

LiCl solutions, although with higher single-channel conductances (Fig. 2). K^+ could also pass through α, β, γ-rENaC, as was observed at concentrations above 1 M. Amiloride effectively blocked α, β, γ-rENaC regardless of the conducting ionic species (data not shown). Even at a decreased signal-to-noise ratio at 3 M KCl, it was still possible to observe discrete channel openings of a finite conductance of 3 pS in magnitude (Fig. 3). This value refers to the highest observed level, since it was not possible to collect meaningful information about subconductive behaviour of the channel when it was conducting K^+. The channel did not pass any detectable Rb^+ or Cs^+ current over a ±120 mV voltage range, at any tested ion concentration (up to 3 M).

Both the single-channel substate (Fig. 4) and the highest conductance state (data not shown) saturated with increasing concentrations of Li^+ or Na^+. However, the conductance *versus* ion concentration plots revealed a conductance maximum at 1 M salt concentration. A conductance maximum was demonstrated for gramicidin (Urban, Hladky & Haydon, 1978; Urban & Hladky, 1979) and inwardly rectifying ROMK1 channels (Lu & MacKinnon, 1994). This was

attributed to 'clogging' with permeant ions when the channel allowed more than one ion into the conduction pathway. In accordance with this idea, an ion channel can be portrayed as a series of potential energy barriers and wells (Läuger, 1973; Hille & Schwartz, 1978), and the conductance data fitted using a parabolic equation (Schumaker & MacKinnon, 1990) of the type:

$$[S^+]/g = (k_B T/z^2 e^2)(A + B[S^+] + C[S^+]^2), \qquad (5),$$

where g is single-channel conductance at ion concentration $[S^+]$, k_B is the Boltzmann constant, z is the valence of ion, e is the elementary charge and T is the absolute temperature. The coefficients A, B and C in eqn (5) are related to the rate constants for ion entry into the channel (a), ion exit (b), and for the ion to hop between binding sites (k) as:

$$A = 2na^{-1},$$

$$B = 2b^{-1} + (n-1)nk^{-1},$$

$$\text{and } C = (n-1)ak^{-1}b^{-1},$$

where n is the number of binding sites within the channel (assumed $n = 2$). This model assumes the existence of
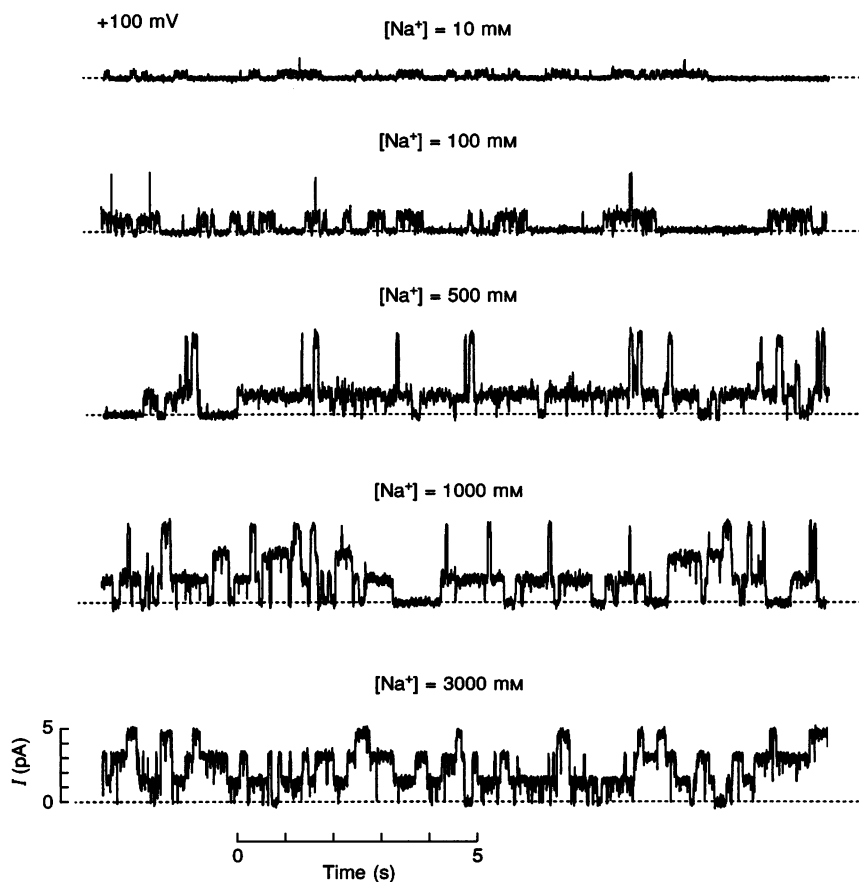

Figure 1. Single-channel records of α, β, γ-rENaC in symmetrical Na^+

Bilayers were bathed with solutions containing NaCl at the concentrations indicated for each trace plus 10 mM Mops–Tris at pH 7·5. Traces shown are sequential and typical of five independent experiments. Holding potential was +100 mV. Current records were filtered at 300 Hz through an 8-pole Bessel filter and acquired at 1 kHz sampling rate using a Digidata 1200 interface and pCLAMP software. For presentation purposes, records were digitally filtered at 100 Hz using pCLAMP software.
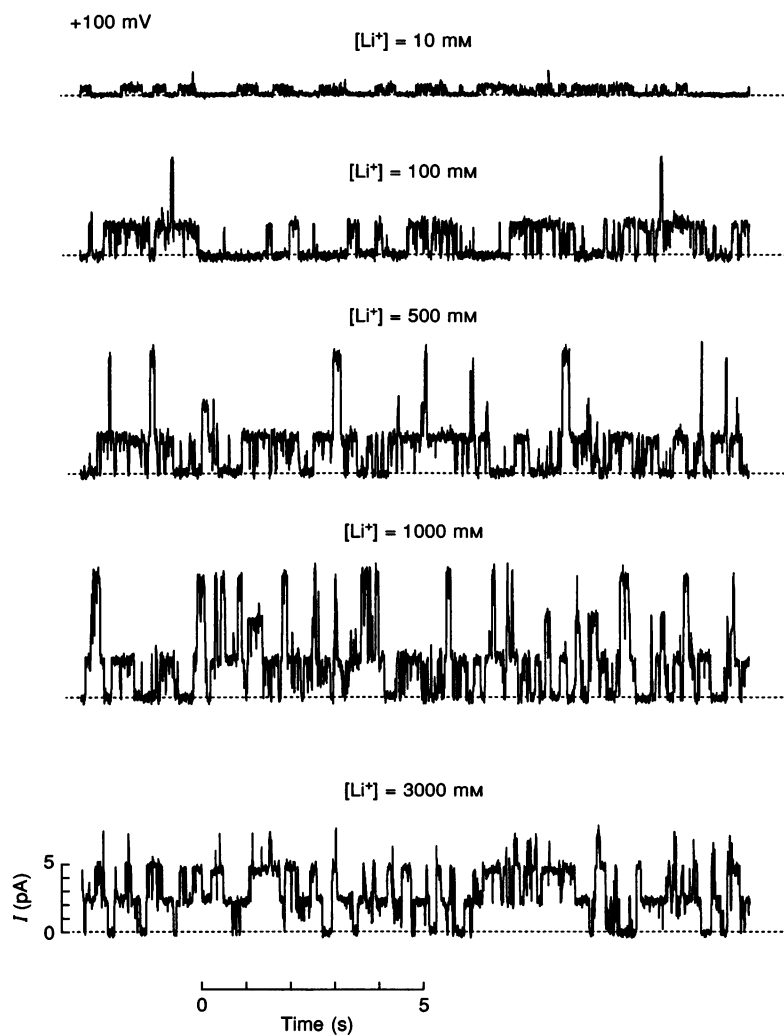
Figure 2. Single-channel records of α, β, γ-rENaC in symmetrical Li⁺

Bilayers were bathed with solutions containing LiCl at the concentrations indicated for each trace plus 10 mM Mops–Tris at pH 7·5. Traces shown are sequential and representative of five experiments. Holding potential was +100 mV. The acquisition and sampling of the records was as indicated in Fig. 1.
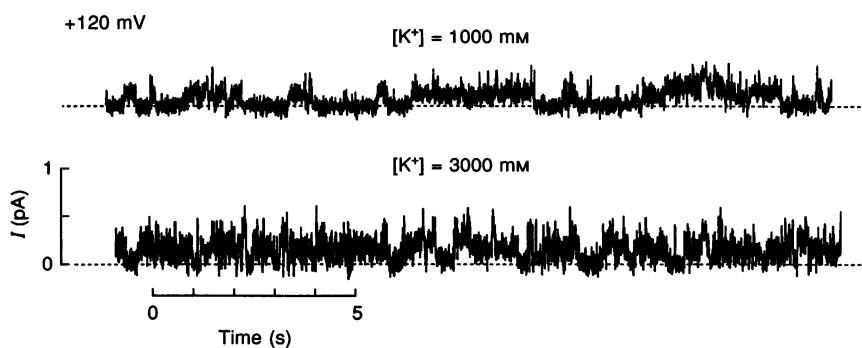

Figure 3. Single-channel records of α, β, γ-rENaC in symmetrical K⁺ solutions

Concentrations of K⁺ in bilayer bathing solution are indicated for each recording. Holding potential was +120 mV. Data acquisition parameters and treatment of the records were as indicated for Fig. 1.
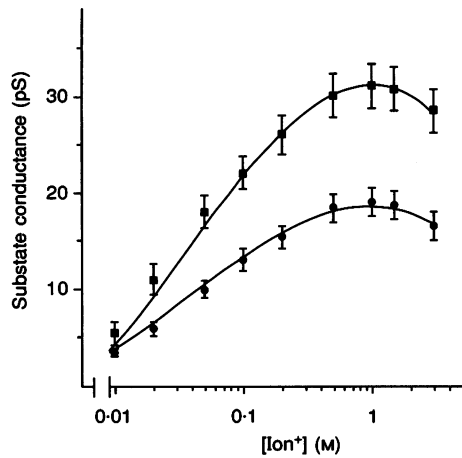
Figure 4. Dependence of α, β, γ-rENaC conductance on [Na$^+$] and [Li$^+$]

Data points and error bars indicate means $\pm$ s.d. for the substate conductance of the α, β, γ-rENaC bathed with Na$^+$-only ($\bullet$) and Li$^+$-only ($\blacksquare$) symmetrical solutions. The continuous curves represent non-linear regression fits using eqn (5) through data points ($N = 7$ and $N = 10$ for Li$^+$ and Na$^+$, respectively). The rate constants obtained from that fit were $a = 2 \cdot 97 \times 10^8$ s^{-1} M^{-1}, $b = 0 \cdot 06 \times 10^8$ s^{-1}, $k = 30 \cdot 6 \times 10^8$ s^{-1}, for Na$^+$, and $a = 3 \cdot 35 \times 10^8$ s^{-1} M^{-1}, $b = 0 \cdot 12 \times 10^8$ s^{-1}, $k = 20 \cdot 8 \times 10^8$ s^{-1}, for Li$^+$.

n sites in the channel with $n - 1$ or n sites always occupied, i.e. there is at least one ion in the channel at any given time. The ratio of rate constants for ion exit (b) and entry (a) yields an ion overall dissociation constant, encompassing all potential binding wells:

$$K_D = b/a. \tag{6}$$

The absolute values of the dissociation constants calculated using eqn (6) were 21 and 35 mM, for Na$^+$ and Li$^+$, respectively. These results suggest that the Na$^+$ energy wells in α, β, γ-rENaC should be deeper than those of Li$^+$.

Figure 5 represents the energy profiles of Na$^+$ and Li$^+$ in α, β, γ-rENaC obtained by fitting the I–V curves at different symmetrical ion concentrations to a three-barrier–two-site (3B2S) model, as a minimal model able to accommodate multiple ion occupancy of the channel, using the AJUSTE program (Alvarez *et al.* 1992). These profiles characterize the channel as one with symmetrical placement of peaks and wells, which is consistent with the symmetrical I–V curves. The heights of external, central and internal

peaks that allow the best fit of I–V curves for Na$^+$ were calculated as 4·8, 10·9 and 4·8 kT, respectively; and for Li$^+$ as 4·5, 10·0 and 4·5 kT, respectively. The depths of both external and internal wells were $-7 \cdot 5$ kT for Na$^+$, and $-6 \cdot 9$ kT for Li$^+$. The finding that the calculated energy wells for Na$^+$ are deeper than the energy wells for Li$^+$ is consistent with the above conclusion based on the analysis of conductance–concentration dependencies. The energy well depths relate to the dissociation constants for individual ions as:

$$K_D = 55 \cdot 5 \exp U, \tag{7}$$

where U is the well energy for the first ion or the well energy for the second ion plus the energy of interaction between ions (the interaction parameter divided by the fraction of the electric field between the two wells). There are 55·5 moles of water in a litre of a solution (true for dilute solutions). Because we used a mole fraction of 1 as the reference state for the ion in solution, the factor of 55·5 moles per litre of solution has to be introduced to
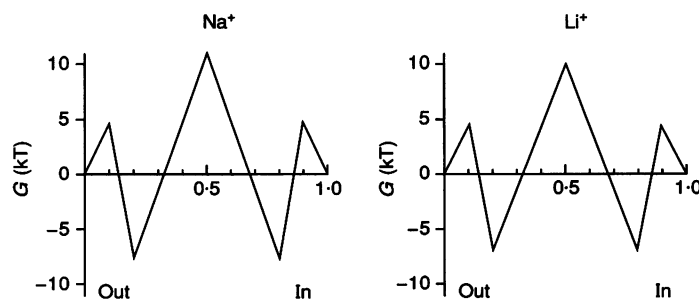

Figure 5. Free energy profiles for Na$^+$ and Li$^+$ in α, β, γ-rENaC

The lines in the graphs represent plots through the points calculated by the AJUSTE computer program for fitting single-channel I–V characteristics of α, β, γ-rENaC bathed with symmetrical NaCl or LiCl solutions. The parameters of the fits were: G1$_{Li}$ = G3$_{Li}$ = 4·5 kT, G2$_{Li}$ = 10·00 kT, U1$_{Li}$ = U2$_{Li}$ = $-6 \cdot 9$ kT, G1$_{Na}$ = G3$_{Na}$ = 4·8 kT, G2$_{Na}$ = 10·9 kT, U1$_{Na}$ = U2$_{Na}$ = $-7 \cdot 5$ kT, D1 = 0·5, D2 = 0·40, D3 = 0·5, D4 = 0·40, D5 = 0·5 and ion interaction parameter = 1·04. The x-axis is expressed in arbitrary units of the electrical field distance within the channel. The extracellular mouth is indicated as zero (Out), and the intracellular mouth (In) as 1·0. The energy (G) is expressed in units of kT, where k is the Boltzmann constant, and T is the absolute temperature.

Figure 6. An anomalous mole fraction effect in α, β, γ-rENaC

The data points represent ratios of single-channel conductances of α, β, γ-rENaC bathed with solutions containing Li^+ and Na^+ at different molar fractions to those in Na^+-only medium. At minimum, five separate experiments were performed for each condition. The dotted lines represent theoretical curves predicted from the energy profiles shown in Fig. 5. The continuous lines represent theoretical curves constructed on the basis of predictions obtained using the refined energy profiles shown in Fig. 7. ●, $[Li^+ + Na^+] = 100$ mM; ■, $[Li^+ + Na^+] = 1000$ mM.
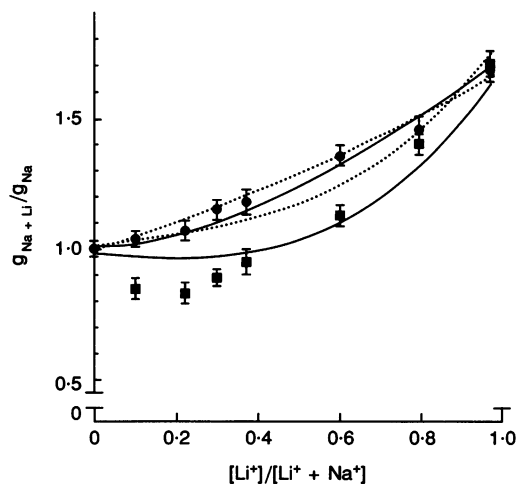
express the binding constant in units of moles per litre. This calculation using the parameters of the Na^+ and Li^+ energy profile (see legend to Fig. 4) gives K_D values for binding of the first Li^+ or Na^+ ion, as 55 and 31 mM, respectively, and 317 and 172 mM for binding of the second ion.

Conductance properties of α, β, γ-rENaC for two permeant ions

The conductance maximum observed with increasing ion concentration is a distinguishing feature of a channel capable of accommodating more than one ion at a time
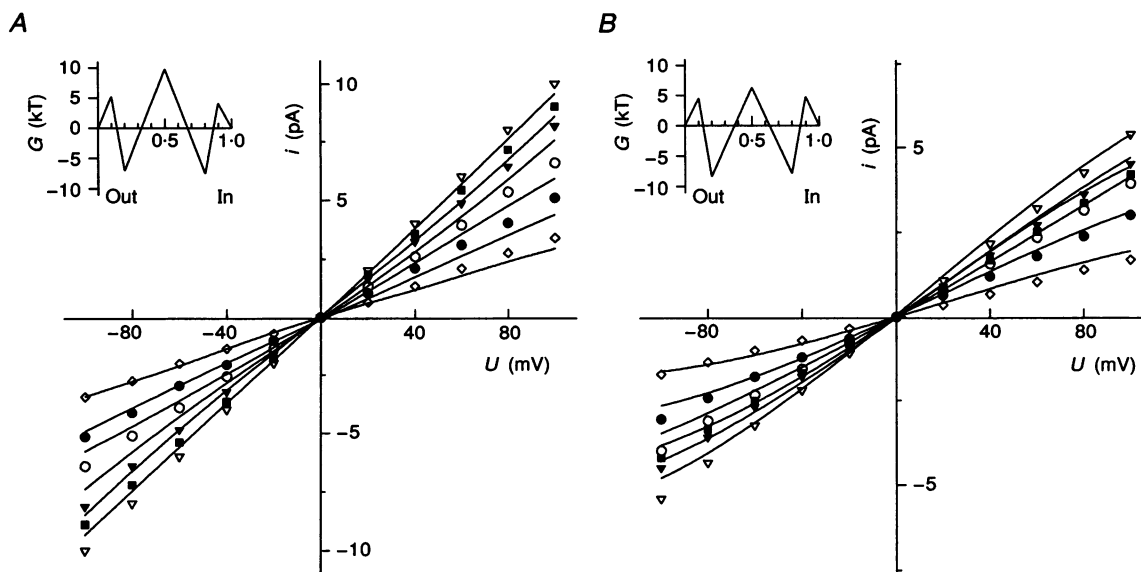
Figure 7. i–V curves of α, β, γ-rENaC bathed with symmetrical LiCl (A) or NaCl solutions (B) at different ionic strengths

Data points represent the means of at least seven separate measurements of the single-channel conductance of α, β, γ-rENaC bathed with symmetrical 20 mM (◇), 50 mM (●), 100 mM (○), 200 mM (▼), 1 M (▽) and 1·5 M (■) NaCl or LiCl solutions. The lines in the graphs represent theoretical i–V curves constructed on the basis of predictions obtained using the energy profiles for Na^+ and Li^+, shown as insets in the respective plots. The energy profiles shown were calculated by AJUSTE computer program for fitting single-channel i–V characteristics of α, β, γ-rENaC bathed with either symmetrical NaCl or LiCl solutions, and with Na^+ and Li^+ solutions at different molar ratios. The parameters of the fits were: $G1_{Li} = 5\cdot2$ kT, $G2_{Li} = 9\cdot7$ kT, $G3_{Li} = 4\cdot0$ kT, $U1_{Li} = -7\cdot0$ kT, $U2_{Li} = -7\cdot5$ kT, $G1_{Na} = 4\cdot5$ kT, $G2_{Na} = 6\cdot3$ kT, $G3_{Na} = 4\cdot8$ kT, $U1_{Na} = -8\cdot3$ kT, $U2_{Na} = -7\cdot8$ kT and ion interaction parameter $= 0\cdot62$. The placements of wells and peaks were the same as in Fig. 5. The x-axis is expressed in arbitrary units of the electrical field distance within the conduction pathway. The extracellular mouth is indicated as zero (Out), and the intracellular mouth (In) as $1\cdot0$. The energy (G) is expressed in units of kT, where k is the Boltzmann constant, and T is the absolute temperature.

(Hille & Schwartz, 1978). Prompted by this observation, we next examined if α, β, γ-rENaC displayed an anomalous mole fraction effect in solutions that contained two permeant ions, namely Na^+ and Li^+. If the single-channel conductance in the presence of two permeant ions at a constant total ionic strength is less than that measured when only one ion is present, 'anomalous' behaviour is said to occur. This feature is also considered to be diagnostic of multiple ion occupancy of the channel (Neher, 1975; Eisenman, Sandblom & Neher, 1977; Hille & Schwartz, 1978; Mironov, 1992). Indeed, an anomalous mole fraction effect was evident for α, β, γ-rENaC when the total ion concentration was maintained at 1 M (Fig. 6), thus supporting the hypothesis of multiple ion occupancy of this channel. However, when the total cation concentration was 100 mM, the ratio of conductances monotonically increased with elevating the Li^+ mole fraction from 0 to 1 (Fig. 6). We compared these experimental data with the predictions of the 3B2S model described above. The theoretical curves (Fig. 6) predicted on the basis of the energy profiles of individual ions in α, β, γ-rENaC calculated using the AJUSTE program (Fig. 5) describe satisfactorily the experimental data points at 100 mM (correlation coefficient

$r = 0.997$, $P < 0.001$), but not at 1 M ($r = 0.593$, $P > 0.2$). Therefore, further refinement of the energy profiles of individual ions in the channel was performed using mole fraction data. Because the number of data points representing the mole fraction experiments was small compared with the total number of observations, the statistical weight of the mole fraction data was taken as five times that of the rest of the data points. Figure 7 depicts the energy profiles for Na^+ and Li^+ resulting from this fit. As predicted by Hille & Schwartz (1978), the anomalous conductance minima in the 3B2S model should occur when the energy profile for at least one of the two ions has high barriers at both ends of the channel. The free energy profiles of individual Na^+ or Li^+ ions in α, β, γ-rENaC calculated using the AJUSTE program complex (see Fig. 7) conform to this prediction. The heights of external, central and internal peaks were 4·5, 6·3 and 4·8 kT, respectively, as determined for Na^+, and 5·2, 9·7 and 4·0 kT, respectively, as determined for Li^+. The depths of both external and internal wells were $-8·3$ and $-7·8$ kT, respectively, for Na^+, and $-7·0$ and $-7·5$ kT for Li^+. These energy profiles do predict an anomalous mole fraction behaviour of the channel at 1 M (correlation coefficient $r = 0.864$, $P < 0.03$), but not at
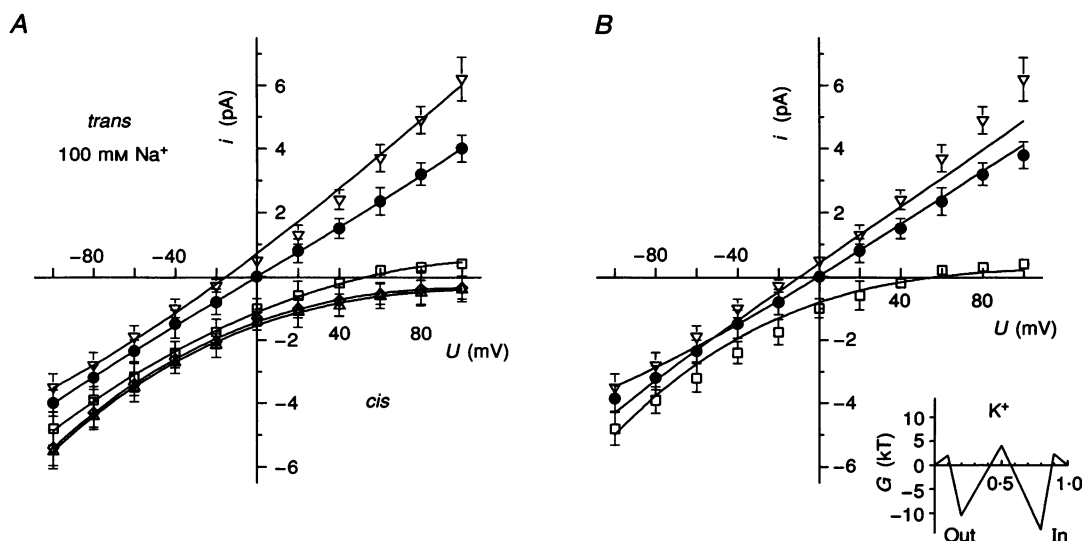

Figure 8. Single-channel current–voltage relationships of α, β, γ-rENaC under biionic conditions

The *trans* compartment always contained 100 mM NaCl and 10 mM Mops–Tris at pH 7·5. The bathing solution in the *cis* compartment contained 100 mM Na^+ (●), 100mM Li^+ (▽), 100 mM K^+ (□), 100 mM Rb^+ (◇) or 100 mM Cs^+ (△), plus 10 mM Mops–Tris at pH 7·5. The data points and error bars represent means ± s.d. for at least four experiments under each condition. Lines through data points represent fits using the Goldman–Hodgkin–Katz equation (eqn 2) (*A*) or by AJUSTE (*B*) using the fixed parameters for Na^+ and Li^+ energy profiles as indicated in Fig. 7. The free energy profile of K^+ in α, β, γ-rENaC (see inset in *B*) was calculated using AJUSTE program under biionic conditions by fitting single-channel i–V characteristics of α, β, γ-rENaC bathed with $NaCl_{trans}$ and KCl_{cis} at different concentrations. Parameters of that fit were: $G1_K = 2·1$ kT, $G2_K = 4·0$ kT, $G3_K = 2·3$ kT, $U1_K = -10·4$ kT, $U2_K = -13·3$ kT and ion interaction parameter $= 1·23$. The placement of peaks and wells, as well as parameters for Na^+ ions were not subjected to fitting and were as indicated in Fig. 7. The x-axis is expressed in arbitrary units of the electrical field distance within the channel. The extracellular mouth is indicated as zero (Out), and the intracellular mouth (In) as 1·0. The energy (*G*) is expressed in units of kT, where k is the Boltzmann constant, and T is the absolute temperature.

Table 1. Biionic reversal potentials of α, β, γ-rENaC in planar lipid bilayers

Ion cis	ψ_{rev}*	$P_S:P_{Na}$ †	N
Li$^+$	$-13\cdot7 \pm 1\cdot5$	$1\cdot72$	5
Na$^+$	$0 \pm 1\cdot0$	1	7
K$^+$	$+55\cdot6 \pm 5\cdot2$	$0\cdot11$	8
Rb$^+$	$+113\cdot7 \pm 6\cdot0$	$0\cdot01$	6
Cs$^+$	$+123\cdot2 \pm 7\cdot2$	$0\cdot007$	7

* ψ_{rev} values were determined by approximation of the biionic I–V curves in the presence of 100 mM NaCl in the *trans* (ground) compartment and 100 mM of the chloride salt of the test cation in the *cis* compartment of the chamber to eqn (2), and corrected for liquid junction potentials. A minimum of five separate measurements were made under each condition. † Calculated using eqn (1) and ψ_{rev}.

100 mM ($r = 0\cdot993$, $P < 0\cdot001$) total cation concentration (Fig. 6). It was important to keep in mind that the parameters of the best fit that could account for the anomalous mole fraction effect still had to describe the single ion data. Indeed, the fit of the single ion I–V curves with the parameters corresponding to the refined energy profiles (Fig. 7) was satisfactory. Hence imposing new constraints for the mole fraction experiments to the fit defines the energy profiles that can account for a larger set of experimental characteristics.

Selectivity properties of α, β, γ-rENaC

We next examined the permeability properties of α, β, γ-rENaC for Li$^+$, Na$^+$ and K$^+$ when these cations were present individually, but at different surfaces of the channel. Figure 8A presents the single-channel i–V

relationships for α, β, γ-rENaC under biionic conditions fitted to the Goldman–Hodgkin–Katz current equation (eqn 2). The relative permeability sequence of α, β, γ-rENaC determined using the biionic reversal potentials (Table 1) was Li$^+$ ($1\cdot72$) > Na$^+$ ($1\cdot00$) > K$^+$ ($0\cdot11$) > Rb$^+$ ($0\cdot01$) > Cs$^+$ ($0\cdot007$) when the *trans* compartment of the chamber contained 100 mM NaCl and the *cis* compartment contained 100 mM chloride salts of the test cation. Lines in the plot (Fig. 8B) represent the theoretical biionic i–V curves constructed by AJUSTE using the fixed parameters for the refined energy profiles of Na$^+$ and Li$^+$ in α, β, γ-rENaC (see Fig. 7). These theoretical i–V curves did not depart much from the experimental data. Moreover, fitting the i–V data under bi-ionic Na$^+$ and K$^+$ conditions by AJUSTE permits the calculation of the energy profile of K$^+$ in α, β, γ-rENaC
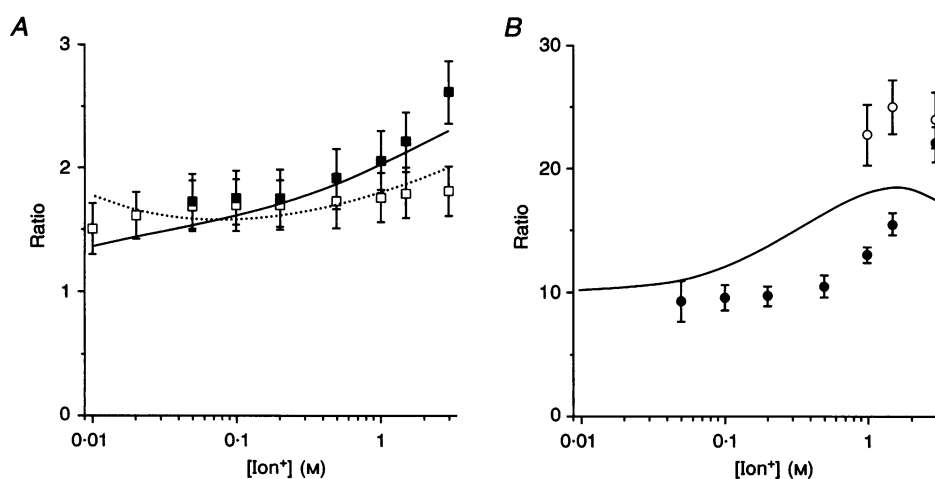

Figure 9. Ion concentration dependence of α, β, γ-rENaC Na$^+$/Li$^+$ and Na$^+$/K$^+$ permeability (P) ratios and single-channel conductance (g) ratios

A, data points and error bars represent means $\pm$ s.d. of at least five separate measurements for each experimental condition. $\square$, g_{Li}/g_{Na}; $\blacksquare$, P_{Li}/P_{Na}. The lines in the graphs represent theoretical i–V curves constructed on the basis of predictions obtained using the energy profiles for Na$^+$ and Li$^+$ shown in Fig. 7 for P_{Li}/P_{Na} ratios (continuous line) and conductance ratios (dotted line). B, data points and error bars represent means $\pm$ s.d. of at least five separate measurements for each experimental condition. $\bigcirc$, g_{Na}/g_K; $\bullet$, P_{Na}/P_K. The lines represent theoretical predictions of the 2S3B model for P_{Na}/P_K ratios (continuous line) obtained using parameters, calculated by the AJUSTE computer program (see inset in Fig. 8).
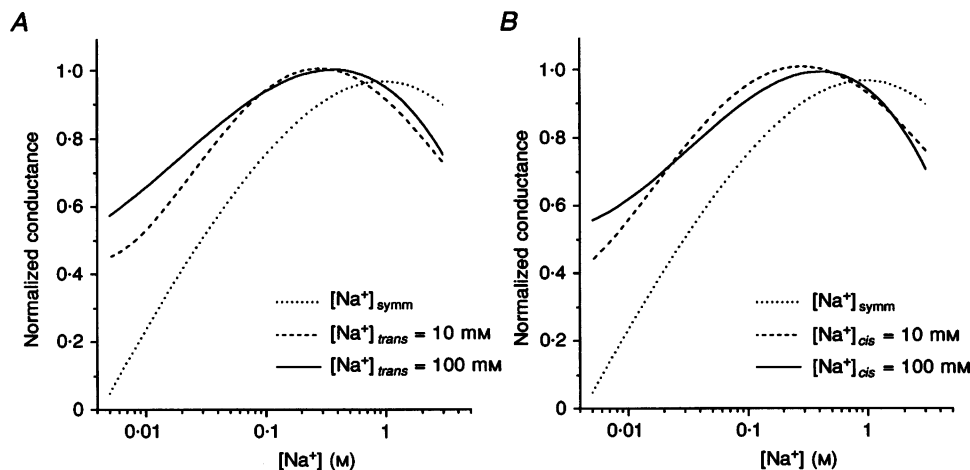
Figure 10. Single channel conductances under different ionic conditions as predicted by the 2S3B model of α, β, γ-rENaC

The lines in the graphs represent the third-order non-linear regressions of the slope conductance data calculated by the AJUSTE program with parameters for the Na^+ energy profile as indicated in Fig. 7, and normalized to the maximum for each curve.

(see inset in Fig. 8B), with the energy peaks of 2·1, 4·0 and 2·3 kT, and the energy wells of $-10·4$ and $-13·3$ kT in magnitude. Solving eqn (7) using the well and ion interaction energies of K^+, and assuming that the distance between the two wells for K^+ is the same as that for Na^+ and Li^+, results in K_D values of 0·6 mM for binding of the first K^+ ion, and 4·3 mM for binding of the second ion. Therefore, based on the Li^+, Na^+ and K^+ energy well depths in α, β, γ-rENaC, the channel binding site affinity sequence for these cations corresponds to $K^+ > Na^+ > Li^+$. Moreover, the relative permeabilities of the channel, calculated from the reversal potentials obtained by non-linear approximation of the biionic i–V curves by AJUSTE, predicted the permeability sequence of α, β, γ-rENaC to be $Li^+ > Na^+ > K^+ > Rb^+ > Cs^+$.

It has also been reported that the ability of a channel to discriminate between ionic species may be dependent on ion concentration, when the channel can hold more than one ion within the conduction pathway (Myers & Haydon, 1972; Begenisich & Cahalan, 1980; Almers & McCleskey, 1984). Figure 9A depicts the results of Li^+/Na^+ relative permeability measurements in α, β, γ-rENaC at different ion concentrations. The P_{Li}/P_{Na} ratio, calculated from the reversal potential measured under biionic conditions, significantly increased with increasing ion concentration, while only a slight increase of the Li^+/Na^+ conductance ratios was observed. Both the theoretical P_{Li}/P_{Na} or the Li^+/Na^+ conductance ratio versus ion concentration curves predicted from the free energy profiles for individual ions as calculated by AJUSTE in the 2S3B model (see Fig. 7) were
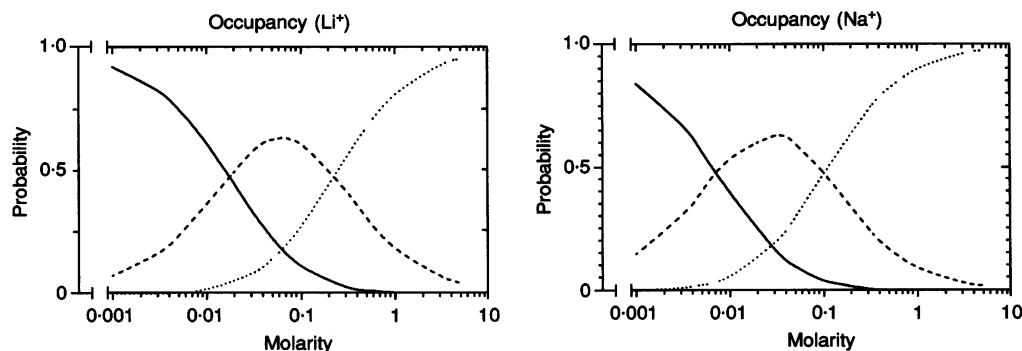

Figure 11. Probability of occupancy of α, β, γ-rENaC by Na^+ or Li^+ as a function of ion concentration

The lines in the graphs represent the third-order non-linear regressions of the occupancy data calculated by the AJUSTE program at 1 mV potential with parameters for the Na^+ and Li^+ energy profiles as indicated in Fig. 7 for the empty channel (continuous line), single occupied channel (dashed line), and double occupied channel (dotted line).

essentially within ± 1 s.d. compared with the experimental data. The ion concentration dependence of Na^+/K^+ selectivity was even more dramatic than that in the case of Li^+ *versus* Na^+. The P_{Na}/P_K ratios calculated from the biionic reversal potentials rose from 9.2 ± 1.4 at 50 mM to 22.9 ± 2.3 at 3 M salt concentration (Fig. 9B). A comparison of the experimental K^+ to Na^+ conductance ratio (Fig. 9B) data (23.0 ± 1.5 at 1 M salt and 24.1 ± 2.7 at 3 M salt) with the predictions based on the free energy profiles for individual ions was precluded by the fact that no defined single-channel current could be measured at K^+ concentrations below 1 M, given the signal-to-noise ratio of the bilayer system. However, the theoretical P_K/P_{Na} *versus* ion concentration curve calculated on the basis of the 2S3B model (Fig. 9B) correlates with the concentration dependence of the measured P_{Na}/P_K ratios. The selectivity data and their correlation with the theoretical curves predicted from the energy profiles for individual ions also support the conclusion that monovalent cation permeation through ENaC can be understood in terms of an energy barrier model featuring two binding sites and three barriers that allows multiple occupancy.

DISCUSSION

Three lines of evidence support the idea that α, β, γ-rENaC behaves as a multi-ion pore: the decrease in conductance at high salt concentration, the anomalous mole fraction behaviour of the channel, and the change in both permeability and conductance ratios for Na^+ and K^+ with increasing ion concentration. The movement of ions through amiloride-sensitive channels was thought to be independent, based on measurements of unidirectional tracer flux ratios in the frog skin (Benos, Hyde & Latorre, 1983), and in the toad urinary bladder (Palmer, 1982) at physiological ionic strengths. In the present experiments, conductance measurements revealed a maximum in both the single α, β, γ-rENaC substate and the highest state conductances at high $[Li^+]$ and $[Na^+]$ (above 1–1.5 M). This finding can be interpreted as self-block of a multi-ion channel, by analogy with the gramicidin A channel (Hladky & Haydon, 1972; Urban *et al.* 1978; Urban & Hladky, 1979), and for both inward and delayed rectifier K^+ channels (Hille & Schwartz, 1978; Lu & MacKinnon, 1994). A conductance maximum was also observed in the early studies in the frog skin (Benos *et al.* 1983). Frehland, Hoshiko & Machlup (1983) proposed a three-state model to explain the sodium concentration dependence of the corner frequency of current noise in response to the blocking agents amiloride and triamterene. The addition of the fourth state to this model helped account for sodium saturation via a two-ion 'clogging' phenomenon, which is in agreement with the conclusion that the epithelial Na^+ channel allows more than one ion to coexist in the conduction pathway.

The analysis of single-channel conductance at different ion concentrations can be performed using the assumption of at least one ion present in the channel at any time. The

dissociation constants for Na^+ and Li^+ calculated as a ratio of the rate constants for ion exit and entry suggest that the affinity of the channel for Na^+ should be higher than that for Li^+. This conclusion is in agreement with the early studies of Palmer & Frindt (1988) who reported a K_D for Na^+ of 25 mM and K_D for Li^+ of 47 mM when they measured the dependence of Na^+ and Li^+ conduction through amiloride-sensitive Na^+ channels on the pipette ion concentration in cell-attached apical membrane patches of rat cortical collecting tubule (CCT) in terms of Michaelis–Menten kinetics. Additionally, they showed that maintaining the ionic strength of the pipette solution at a constant high level resulted in a 2-fold increase in the K_D for both Li^+ (Palmer & Frindt, 1986) and Na^+ (Palmer & Frindt, 1988). A variability in dissociation constants has been reported in the literature for other amiloride-sensitive Na^+ channels studied using different techniques. For example, K_D for Na^+ for amiloride-sensitive sodium channels in A6 cells was in the range of 17–20 mM, when they were either purified and subsequently studied in planar lipid bilayers (Olans, Sariban-Sohraby & Benos, 1984), or examined by the patch-clamp technique (Eaton & Hamilton, 1988). Oh & Benos (1993) measured a K_D for Na^+ of 45–55 mM for immuno-purified bovine renal Na^+ channels reconstituted into lipid bilayers. Furthermore, for this channel, the apparent Na^+ dissociation constant decreased from ~45 mM, when Na^+ was varied on both sides of the channel simultaneously, to ~10 mM, when Na^+ was varied only on one (either *cis* or *trans*) side (Ismailov, Berdiev & Benos, 1995). Since the apparent K_D values calculated from the single-channel conductance–concentration analyses in terms of the Michaelis–Menten kinetics do not always give a true measure of the equilibrium constant(s), we investigated the theoretical ion concentration dependencies of the single-channel conductance predicted on the basis of the 2S3B model developed for α, β, γ-rENaC (Fig. 10). The curves were obtained by calculating currents for the channel with the Na^+ energy profile as shown in Fig. 7 under different ionic conditions, namely when varying $[Na^+]_{cis}$, but not $[Na^+]_{trans}$ (Fig. 10A), and when varying $[Na^+]_{trans}$, but not $[Na^+]_{cis}$ (Fig. 10B). In all cases, the model predicts a conductance maximum, with an obvious leftward shift of the curves compared with the theoretical conductance/ion concentration curve when both $[Na^+]_{cis}$ and $[Na^+]_{trans}$ were set as variables. This demonstrates that the shift in K_D values observed in symmetrical *versus* fixed *trans* or *cis* concentration experiments is a feature of the conduction model rather than a true change in channel structure. Moreover, the curve generated for the ionic conditions presumably used in the early experiments of Benos *et al.* (1983), namely 10 mM $[Na^+]_{cis}$ and variable $[Na^+]_{trans}$ (Fig. 10B), indeed predicts a conductance maximum at physiological ion concentrations. On the other hand, the same energy profiles of Na^+ and Li^+ in ENaC predict an anomalous mole fraction behaviour of the channel at 1 M, but not at 100 mM, total cation concentration (Fig. 6), suggesting that, at physiological ion concentrations,

Table 2. Comparison of relative ion selectivities of α, β, γ-rENaC determined by conductances and biionic potentials

Ion	g_S/g_{Na^+} (1000 mM)*	P_S/P_{Na^+} (1000 mM)†
Li^+	1.63 ± 0.21	2.05 ± 0.24
K^+	0.040 ± 0.005	0.076 ± 0.005

A minimum of five separate measurements were made using each method. * Ratio of single α,β,γ-rENaC conductances in the presence of symmetrical 1 M solutions of the chloride of the test cation. † Calculated using eqn (1) and ψ_{rev} measured in the presence of 1 M of NaCl in the *trans* and 1 M of the chloride salt of the test cation in the *cis* compartment of the chamber.

α,β,γ-rENaC may be singly occupied, or empty. This possibility is illustrated in the plot of ion occupancy of the channel calculated by AJUSTE in the low limit of holding potential (1 mV to approximate the zero voltage condition) for different concentrations of Li^+ and Na^+ (Fig. 11). The concentration at which a channel featuring two binding sites, three barriers, and allowing double occupancy, is occupied by one ion with a probability of 50%, can be determined from these plots (7.3 and 3.6 mM for Li^+ and Na^+, respectively), and is clearly related to the thermodynamic concept of the binding constant.

However, in our experiments the channel conductance maximum does not appear unless the concentration of a permeant cation reaches 1 M. That finding can be accounted for by the electrostatic ion repulsion effects in ENaC, which should follow Coulomb's law as:

$$A \approx (N_A z_1 z_2 e^2)/(4\pi \epsilon \epsilon_0 \sigma), \qquad (8)$$

where N_A is Avogadro's constant, z_1 and z_2 are the valencies of two ions placed at the distance σ, e is the elementary charge, and ϵ and ϵ_0 are the dielectric constants of the surrounding medium and vacuum, respectively (assuming the pore is an infinite homogenous medium). Equation (8) illustrates that the physical significance of the interaction parameter in this case should be related to the dielectric constant of the surrounding medium, whereas the ultimate result of ion repulsion is to affect the affinities of binding sites for the ions (for discussion, see Hille & Schwarz, 1978; Levitt, 1978; Almers & McCleskey, 1984, Hess & Tsien, 1984). Therefore, the ion rate constants are related to ion repulsion in a way that the exit rate constant for ions leaving a doubly occupied pore increases. Based on the results of the calculation using eqn (7), we conclude that ion repulsion causes a 5-fold decrease in affinity of the second binding site, when the first site is occupied. Depending on the assumed dielectric constant inside the channel, the assumed charge separation distance, and the valencies of the interacting ions, this factor can be expected within the range of 2–20 000 for different multi-ion channels (Hille & Schwartz, 1978; Almers & McCleskey, 1984; Hess & Tsien, 1984). Therefore in ENaC the electrostatic interaction between two ions can be greatly attenuated due to a high

dielectric constant of the medium inside the channel and/or due to a large distance between binding sites. The first possibility is supported by the finding that ENaC can accommodate up to two water molecules (Ismailov, Shlyonsky & Benos, 1997b). Furthermore, a flux ratio exponent of 1 found in the frog skin (Benos et al. 1983), and in the toad bladder (Palmer, 1982) can be expected in the multi-ion channel featuring the central energy barrier higher than the lateral barriers with a low ion repulsion (Hille, 1992).

Although Li^+ and Na^+ are the major permeant ions for α,β,γ-rENaC, a finite K^+ conductance of this channel (3.1 ± 0.4 pS) was measured at K^+ concentrations above 1 M. Two possibilities could account for this observation, because K^+ impermeability has become one of the distinguishing 'hallmarks' of epithelial Na^+ channels (Palmer & Frindt, 1988; Canessa et al. 1994). First, the ion selectivity of the channel can be calculated either from the biionic reversal potentials using the Goldman–Hodgkin–Katz voltage equation, or as a ratio of the single-channel conductances for two different ions measured under similar conditions. It has been shown for some channels that the selectivities calculated using these methods may differ by an order of magnitude (Myers & Haydon, 1972; Coronado, Rosenberg & Miller, 1980). Second, it has also been reported that the selectivity of multi-ion channels is dependent on ion concentration in the bathing solution (Myers & Haydon, 1972; Begenisich & Cahalan, 1980; Almers & McCleskey, 1984). Our measurements were performed using both methods (Table 2). Both the P_{Li}/P_{Na} and P_K/P_{Na} ratios calculated from biionic reversal potentials were quite different from the ratios of the channel conductances for individual ions, and displayed strong ion concentration dependence. The free energy profiles for the individual ions as calculated by AJUSTE in the 2S3B model (see Figs 7 and 8) predicted theoretical curves for conductance/ion concentration dependencies that were in good agreement with the experimental data (Fig. 9). Although the 2S3B theory fails to reproduce the details of the experimental curve, it is evident that experimental and theoretical permeability ratios move in the same direction.

To summarize, the predictions of a model featuring three energy barriers, two binding sites, and allowing double occupancy developed for α, β, γ-rENaC on the basis of single ion I–V relationships are in agreement with the observed conductance maximum in single ion experiments, conductance minimum in the mole fraction experiments, non-linearity of the I–V curves in biionic experiments, and the concentration dependence of the permeability ratios. Moreover, computer simulations performed using this model provide insights into the nature of (i) the sidedness of ion concentration dependencies of single-channel conductance observed in the immunopurified bovine renal amiloride-sensitive Na⁺ channel, i.e. a difference in the K_D values for Na⁺ when varied at one side of the channel *versus* that when [Na⁺] is varied at both sides (Ismailov *et al.* 1995); and (ii) a conductance maximum, albeit with unitary tracer flux ratios observed in the frog skin (Benos *et al.* 1983) and in the toad urinary bladder (Palmer, 1982) at physiological ionic strengths. Taken together, these results support our hypothesis that ENaCs form a core conduction unit of epithelial Na⁺ channels (Ismailov, Berdiev, Bradford, Awayda, Fuller & Benos, 1996 *b*).

ALMERS, W. & MCCLESKEY, E. W. (1984). Non-selective conductance in calcium channels of frog muscle: calcium selectivity in a single-file pore. *Journal of Physiology* **353**, 585–608.

ALVAREZ, O., VILLARROEL, A. & EISENMAN, G. (1992). Calculation of ion currents from energy profiles and energy profiles from currents in multibarrier, multisite, multi-occupancy channel model. *Methods in Enzymology* **207**, 816–854.

AWAYDA, M. S., ISMAILOV, I. I., BERDIEV, B. K. & BENOS, D. J. (1995). A cloned renal epithelial Na⁺ channel protein displays stretch activation in planar lipid bilayers. *American Journal of Physiology* **268**, C1450–1459.

BEGENISICH, T. B. & CAHALAN, M. D. (1980). Sodium channel permeation in squid axon. I. Reversal potential experiments. *Journal of Physiology* **307**, 217–242.

BENOS, D. J., HYDE, B. A. & LATORRE, R. (1983). Sodium flux ratio through the amiloride-sensitive entry pathway in frog skin. *Journal of General Physiology* **81**, 667–685.

CANESSA, C. M., HORISBERGER, J.-D. & ROSSIER, B. C. (1993). Epithelial sodium channel related to proteins involved in neurodegeneration. *Nature* **361**, 467–470.

CANESSA, C. M., SCHILD, L., BUELL, G., THORENS, B., GAUTSCHI, I., HORISBERGER, J.-D. & ROSSIER, B. C. (1994). Amiloride-sensitive epithelial Na⁺ channel is made of three homologous subunits. *Nature* **367**, 463–466.

CORONADO, R., ROSENBERG, R. L. & MILLER, C. (1980). Ionic selectivity, saturation, and block in a K⁺-selective channel from sarcoplasmic reticulum. *Journal of General Physiology* **76**, 425–446.

EATON, D. C. & HAMILTON, K. L. (1988). The amiloride-blockable sodium channel of epithelial tissue. In *Ionic Channels*, vol. 1, ed. NARAHASHI, T., pp. 251–282. Plenum Press, New York.

EISENMAN, G., LATORRE, R. & MILLER, C. (1986). Multi-ion conduction and selectivity in the high-conductance Ca²⁺-activated K⁺ channel from skeletal muscle. *Biophysical Journal* **50**, 1025–1034.

FREHLAND, E., HOSHIKO, T. & MACHLUP, S. (1983). Competitive blocking of apical sodium channels in epithelia. *Biochimica et Biophysica Acta* **732**, 636–646.

FULLER, C. M., AWAYDA, M. S., ARRATE, P., BRADFORD, A., MORRIS, R. G., CANESSA, C. M., ROSSIER, B. C. & BENOS, D. J. (1995). Cloning of a bovine epithelial Na⁺ channel subunit. *American Journal of Physiology* **269**, C641–654.

HESS, P. & TSIEN, R. W. (1984). Mechanism of ion permeation through calcium channels. *Nature* **309**, 453–456.

HILLE, B. (1992). *Ionic Channels of Excitable Membranes*, 2nd edition. Sinauer Associates, Inc., Sunderland, MA, USA.

HILLE, B. & SCHWARTZ, W. (1978). Potassium channels as multi-ion single-file pores. *Journal of General Physiology* **72**, 409–442.

HLADKY, S. B. & HAYDON, D. A. (1972). Ion transfer across lipid membranes in the presence of gramicidin A. I. Studies of the unit conductance channel. *Biochimica et Biophysica Acta* **274**, 294–312.

ISMAILOV, I. I., AWAYDA, M. S., BERDIEV, B. K., BUBIEN, J. K., LUCAS, J. E., FULLER, C. M. & BENOS, D. J. (1996 *a*). Triple-barrel organization of ENaC, a cloned epithelial Na⁺ channel. *Journal of Biological Chemistry* **271**, 807–816.

ISMAILOV, I. I., BERDIEV, B. K. & BENOS, D. J. (1995). Regulation by Na⁺ and Ca²⁺ of renal epithelial Na⁺ channels reconstituted into planar lipid bilayers. *Journal of General Physiology* **106**, 445–466.

ISMAILOV, I. I., BERDIEV, B. K., BRADFORD, A. L., AWAYDA, M. S., FULLER, C. M. & BENOS, D. J. (1996 *b*). Associated proteins and renal epithelial Na⁺ channel function. *Journal of Membrane Biology* **149**, 123–132.

ISMAILOV, I. I., BERDIEV, B. K., SHLYONSKY, V. G. & BENOS, D. J. (1997 *a*). Mechanosensitivity of a cloned epithelial Na⁺ channel: Release from Ca²⁺ block. *Biophysical Journal* **72**, 1182–1192.

ISMAILOV, I. I., SHLYONSKY, V. GH. & BENOS, D. J. (1997 *b*). Streaming potential measurements in $\alpha\beta\gamma$-rENaC in planar lipid bilayers. *Proceedings of the National Academy of Sciences of the USA* **94**, 7651–7654.

LÄUGER, P. (1973). Ion transport through pores a rate-theory analysis. *Biochimica et Biophysica Acta* **311**, 423–441.

LEVITT, D. G. (1978). Electrostatic calculations for an ion channel. I. Energy and potential profiles and interactions between ions. *Biophysical Journal* **22**, 209–219.

LIDE, D. R. (1996). *Handbook of Chemistry and Physics*, 77th edition, pp. 5100–5106. CRC Press, Inc.

LINGUEGLIA, E., VOILLEY, N., WALDMAN, R., LAZDUNSKI, M. & BARBRY, P. (1993). Expression cloning of an epithelial amiloride sensitive Na⁺ channel. A new channel type with homologies to *Caenorhabditis elegans* degenerins. *FEBS Letters* **318**, 95–99.

LU, Z. & MACKINNON, R. (1994). A conductance maximum observed in an inward-rectifier potassium channel. *Journal of General Physiology* **104**, 477–486.

MIRONOV, S. L. (1992). Conformational model for ion permeation in membrane channels: A comparison with multi-ion models and applications to calcium channel permeability. *Biophysical Journal* **63**, 487–496.

MYERS, V. B. & HAYDON, D. A. (1972). Ion transfer across lipid membranes in the presence of gramicidin A. II. The ion selectivity. *Biochimica et Biophysica Acta* **274**, 313–322.

NEHER, E. (1975). Ionic specificity of the gramicidin channel and the thallous ion. *Biochimica et Biophysica Acta* **401**, 540–544.

OH, Y. & BENOS, D. J. (1993). Single-channel characteristics of a purified bovine renal amiloride-sensitive Na⁺ channel in planar lipid bilayers. *American Journal of Physiology* **264**, C1489–1499.

OLANS, L., SARIBAN-SOHRABY, S. & BENOS, D. J. (1984). Saturation behavior of single, amiloride sensitive Na$^+$ channels in planar lipid bilayers. *Biophysical Journal* **46**, 831–835.

PALMER, L. G. (1982). Na$^+$ transport and flux ratio through apical Na$^+$ channels in toad bladder. *Nature* **297**, 688–690.

PALMER, L. G. & FRINDT, G. (1986). Amiloride sensitive channels from the apical membrane of the rat cortical collecting tubule. *Proceedings of the National Academy of Sciences of the USA* **83**, 2767–2770.

PALMER, L. G. & FRINDT G. (1988). Conductance and gating of epithelial Na channels from rat cortical collecting tubule. Effects of luminal Na and Li. *Journal of General Physiology* **92**, 121–138.

PUOTI, A., MAY, A., CANESSA, C. M., HORISBERGER, J.-D., SCHILD, L. & ROSSIER, B. C. (1995). The highly selective low-conductance epithelial Na$^+$ channel of *Xenopus laevis* A6 kidney cells. *American Journal of Physiology* **269**, C188–197.

SCHUMAKER, M. F. & MACKINNON, R. (1990). A simple model for multi-ion permeation. Single-vacancy conduction in a simple pore model. *Biophysical Journal* **58**, 975–984.

TIEN, H. T., CARBONE, S. & DAWIDOWICZ, E. A. (1966). Formation of 'black' lipid membranes by oxidation product of cholesterol. *Nature* **215**, 1199–1200.

URBAN, B. W. & HLADKY, S. B. (1979). Ion transport in the simplest single file pore. *Biochimica et Biophysica Acta* **554**, 410–429.

URBAN, B. W., HLADKY, S. B. & HAYDON, D. A. (1978). The kinetics of ion movements in the gramicidin channel. *Federation Proceedings* **37**, 2628–2632.

Author's email address

I. I. Ismailov: Ismailov@PhyBio.bhs.uab.Edu